0013-7227/06/$15.00/0
Printed in U.S.A.

Endocrinology 147(9):4160–4168

doi: 10.1210/en.2006-0251

Insulin Resistance Accelerates Muscle Protein Degradation: Activation of the Ubiquitin-Proteasome Pathway by Defects in Muscle Cell Signaling

Xiaonan Wang, Zhaoyong Hu, Junping Hu, Jie Du, and William E. Mitch

Renal Division (X.W., J.H.), Department of Medicine, Emory University, Atlanta, Georgia 30322; and Nephrology Division (Z.H., J.D., W.E.M.), Baylor College of Medicine, Houston, Texas 77030

Conditions such as acidosis, uremia, and sepsis are characterized by insulin resistance and muscle wasting, but whether the insulin resistance associated with these disorders contributes to muscle atrophy is unclear. We examined this question in *db/db* mice with increased blood glucose despite high levels of plasma insulin. Compared with control littermate mice, the weights of different muscles in *db/db* mice and the cross-sectional areas of muscles were smaller. In muscle of *db/db* mice, protein degradation and activities of the major proteolytic systems, caspase-3 and the proteasome, were increased. We examined signals that could activate muscle proteolysis and found low values of both phosphatidylinositol 3 kinase (PI3K) activity and phosphorylated Akt that were related to phosphorylation of serine 307 of insulin receptor substrate-1. To assess how changes in circulating insulin and glucose affect muscle protein, we treated *db/db* mice with rosiglitazone. Rosiglitazone improved indices of insulin resistance and abnormalities in PI3K/Akt signaling and decreased activities of caspase-3 and the proteasome in muscle leading to suppression of proteolysis. Underlying mechanisms of proteolysis include increased glucocorticoid production, decreased circulating adiponectin, and phosphorylation of the forkhead transcription factor associated with increased expression of the E3 ubiquitin-conjugating enzymes atrogin-1/MAFbx and MuRF1. These abnormalities were also corrected by rosiglitazone. Thus, insulin resistance causes muscle wasting by mechanisms that involve suppression of PI3K/Akt signaling leading to activation of caspase-3 and the ubiquitin-proteasome proteolytic pathway causing muscle protein degradation. (*Endocrinology* 147: 4160–4168, 2006)

LOSS OF PROTEIN stores and a decline in lean body mass are associated with morbidity and mortality, making this a major clinical problem (1–4). There is evidence that loss of lean body mass is usually caused by activation of the ubiquitin-proteasome proteolytic pathway (UPP) in muscle (5), but the pathophysiological triggers that accelerate protein degradation are controversial. Inflammation is often suggested as a trigger because many illnesses causing loss of lean body mass are associated with increases in circulating cytokines (6–8). However, inflammation can be linked to insulin resistance because high levels of circulating TNFα and possibly other cytokines can cause insulin resistance (9, 10). Another potential proteolytic trigger of muscle protein breakdown is a decrease in the responses to insulin or IGF-I. For example, there is evidence that insulin deficiency causes muscle protein breakdown by activating the UPP in processes that include transcription of genes encoding subunits of this system (11, 12). This is relevant because catabolic conditions that stimulate muscle protein degradation by the UPP such as aging, acidosis, chronic kidney disease (CKD), or acidosis are often associated with insulin resistance (13–16). The presence of these complicating factors raises the question of whether insulin resistance by itself will stimulate protein metabolism and, if so, by what mechanisms.

In a model of insulin deficiency, we showed that there is accelerated muscle proteolysis and that this is caused by a decrease in the activity of phosphatidylinositol 3-kinase (PI3K) (17, 18). We found that a decrease in PI3K activity reduces the level of phosphorylated Akt (pAkt), and a low pAkt has been shown to relieve the inhibition of the expression of specific E3 ubiquitin-conjugating enzymes atrogin-1/MAFbx and MuRF1 in muscle (17, 19, 20). This is relevant because expression of these E3 enzymes occurs in several conditions causing loss of lean body mass, suggesting there is a complex genetic program associated with activation of muscle protein degradation (21). Besides stimulating activity of the UPP, we found that a decrease in muscle PI3K activity also activates Bax, which stimulates the activity of caspase-3 leading to muscle protein loss by providing substrates for the UPP (17, 18).

In the present study, we explored the possibility that insulin resistance would cause muscle atrophy and examined potential proteolytic pathways that could cause accelerated loss of muscle protein. We took advantage of the well-established characteristics of *db/db* mice to test this possibility because kidney failure, systemic sepsis, *etc.* do not complicate this genetic model of insulin resistance. Thus, *db/db* mice provided us an opportunity to determine whether insulin resistance alone can stimulate the UPP and muscle protein degradation.

First Published Online June 15, 2006

Abbreviations: AMC, 7-Amino-4-methylcoumarin; CKD, chronic kidney disease; EDL, extensor digitorum longus; GAPDH, glyceraldehyde-3-phosphate dehydrogenase; pAkt, phosphorylated Akt; PI3K, phosphatidylinositol 3 kinase; UPP, ubiquitin-proteasome pathway.

***Endocrinology* is published monthly by The Endocrine Society (http://www.endo-society.org), the foremost professional society serving the endocrine community.**

Materials and Methods

Animals

We studied *db/db* mice (BKS.Cg-m +/+Lepr <db>; Jackson Laboratories, Bar Harbor, ME), and wild-type (WT) (C57BLKS/J <m+/m+>) littermates were studied as controls. The experiments were approved by the institutional animal care and use committee of Emory University. Four-week-old male *db/db* and control mice were housed in the animal care facility in 12-h light, 12-h dark cycles and fed *ad libitum*. In one experiment, mice were placed in metabolic cages to collect a 24-h urine sample, and corticosterone excretion was measured (R&D Systems, Minneapolis, MN) to estimate glucocorticoid production (12). In another experiment, mice were fed the standard or a diet supplemented with rosiglitazone maleate (8 mg/kg·d; GlaxoSmithKline, Pittsburgh, PA).

At the end of different experimental manipulations, *db/db* and control mice were anesthetized with 12 mg/kg xylazine and 60 mg/kg ketamine, and the soleus, the extensor digitorum longus (EDL), and plantaris muscles were removed to measure protein degradation; gastrocnemius muscles were also removed, plunged into liquid nitrogen, and stored at −80 C.

Plasma insulin was measured using 1–2-3 ultrasensitive mouse insulin enzyme immunoassay (EIA) kit (American Lab Products, Windham, NH) by the Biochemistry Core Laboratory of Emory University. Blood glucose concentration was measured by the Accu-CHEK advantage blood glucose meter (Indianapolis, IN). Adiponectin concentration in serum was measured using a mouse adiponectin ELISA kit (American Lab Products).

Protein degradation

Protein degradation was measured as the rate of tyrosine release into the media because muscle neither synthesizes nor degrades tyrosine and it does not accumulate in the intracellular pool (22, 23). Soleus, EDL, and plantaris muscles were pinned to plastic supports to maintain muscles at resting length. They were incubated in standard Krebs-Henseleit bicarbonate buffer containing 10 mM glucose and 0.5 mM cycloheximide (to block tyrosine reuse), placed in individual flasks, and gassed with 95% O_2/5% CO_2 for 3 min. After an initial 30-min preincubation, each muscle was transferred to a flask containing fresh media, regassed with 95% O_2/5% CO_2 for 3 min, and incubated at 37 C for 2 h. Tyrosine in the media was measured (5, 22).

Immunoblotting

Gastrocnemius muscles were homogenized in RIPA buffer except when we measured the 14-kDa actin fragment arising from the activity of caspase-3 (18). To measure this actin fragment, muscles were harvested and homogenized in hypotonic buffer and protein concentration was measured using a PC protein assay kit (Bio-Rad, Hercules, CA). The levels of signaling proteins and the 14-kDa actin fragment were detected by standard Western blotting (17, 18). We used the following primary antibodies: an antiactin antibody (Sigma-Aldrich, St. Louis, MO), an anti-IRS-1 antibody (Upstate, Lake Placid, NY), and Cell Signaling (Danvers, MA) antibodies against phospho-Ser307 IRS-1, Akt, pAkt, and the forkhead transcription factors, FoxO1 and pFoxO1.

Muscle histology

To assess differences in the cross-sectional area of the plantaris muscle, we embedded them in TBS tissue freezing media (Fisher, Pittsburgh, PA) in isopentane cooled in dry ice. Cross-sections (10 μm) on gelatin-coated slides were treated with an anti-laminin antibody (Sigma-Aldrich), and the area of at least 500 individual myofibers per muscle was measured using the Micro-Suite Five Biological System (Olympus, Melville, NY).

Proteasome activity

To measure proteasome chymotryptic-like peptidase activity *in vitro*, gastrocnemius muscles were homogenized in a harvest buffer [50 μM Tris-HCl (pH 7.4), 5 mM $MgCl_2$, 250 mM sucrose, 2 mM ATP, and 1 mM dithiothreitol]. The mixture was centrifuged (5 min at 400 × *g*) and clarified by sequential centrifugations of 10,000 × *g* for 20 min before centrifuging at 100,000 × *g* for 5 h to isolate the 20S and 26S proteasomes (24). After resuspension, proteasome chymotryptic-like activity was determined as the release of 7-amino-4-methylcoumarin (AMC) from the fluorogenic peptide substrate LLVY-AMC (*N*-Suc-Leu-Leu-Val-Tyr-AMC) using the Proteasome Activity Assay Kit (Chemicon International, Temecula, CA).

Cell culture and RT-PCR

Mouse 3T3-L1 preadipocytes, purchased from American Type Culture Collection (Manassas, VA) were studied between passages 3 and 10. Initially, they were grown in standard media containing DMEM (Invitrogen, Carlsbad, CA) containing 10% bovine calf serum (HyClone, Logan, UT), penicillin (200 U/ml), and streptomycin (200 μg/ml) in a humidified atmosphere (95% O_2/5% CO_2). After 2 d, cells were switched to differentiation media with 1 μM dexamethasone, 10 μg/ml insulin, and 0.5 mM 3-methyl-1-isobutylxanthine (Sigma-Aldrich) for 2 d and then grown in post-differentiation medium containing 10 μg/ml insulin for 5 d. Before being studied, cells were shown to be maximally differentiated morphologically (>90% of cells). The cells were then placed in standard media for another 2 d. Subsequently, we determined the influence of exposing cells to 10 μM rosiglitazone (Cayman Chemical, Ann Arbor, MI) for 16 h.

For measuring RT-PCR, we isolated total RNA from mouse muscles and from differentiated 3T3-L1 cells using Trizol reagent (Invitrogen). RT was performed using the GeneAmp RNA PCR Core kit (Applied Biosystems, Foster City, CA) and 2 μg denatured RNA according to the manufacturer's instructions. Primers for specific genes were designed to cross intron-exon boundaries and used to generate amplicons in their linear ranges as follows: adiponectin (U37222; 532-bp product), forward, 5′-GATTCAACTTGCGCCTCATCTTAGGC-3′, and reverse, 5′-CCGACGTTACTACAACTGAAGAGC-3′; TNFα (NM_11731; 212-bp product), forward, 5′-TCTCATCAGTTCTATGGCCC-3′, and reverse, 5′-GGGAGTAGACAAGGTACAAC-3′; and IL-6 (NM_031168; 343-bp product), forward, 5′-GCCAGAGTCCTTCAGAGAGATACAG-3′, and reverse, 5′-CCCAAC**G**ATTCATATTGTCAG-3′. For each sample, 18S rRNA was used as an internal control using QuantumRNA 18S primers (Ambion, Austin, TX).

Real-time PCR

Total RNA was extracted using the Purelink RNA purification kit (Invitrogen) and 2 μg RNA sample was used for RT by oligo 9-mer primers and Superscript II (Invitrogen). Real-time PCR was performed with SYBR Green PCR reagents (Bio-Rad, Hercules, CA) and the Opticon DNA Engine (Bio-Rad) using the following cycle parameters: 94 C for 2 min and 40 cycles at 94 C for 15 sec, 55 C for 30 sec, and 72 C for 30 sec with a final extension at 72 C for 10 min. Primers used in this study were mouse atrogin-1/MAFbx, forward, 5′-GCAGAGAGTCGGCAAGTC-3′, and reverse, 5′-CAGGTCGGTGAT CGTGAG-3′; mouse MuRF-1, forward, 5′-CAACCTGTGCCGCAAGTG-3′, and reverse, 5′-CAACCTCGT GCCTACAAGATG-3′; and mouse glyceraldehyde-3-phosphate dehydrogenase (GAPDH), forward, 5′-ACCCCCAATGTAT CCGTTGT-3′, and reverse, 5′-TACTCCTTGGAGGCCATGTA-3′. The threshold cycle (Ct) is defined as the number of cycles required for the fluorescence signal to exceed the detection threshold. mRNA expression was standardized to the GAPDH gene, and expression was calculated as the difference between the threshold values of the two genes ($2^{-\Delta Ct}$). Melting curve analysis was always performed during real-time quantitative PCR to analyze and verify the specificity of the reaction. The values are given as the means ± SE of three independent experiments.

Statistical analysis

Results are presented as mean ± SE. Comparisons of results between groups were by ANOVA using Systat Software ANOVA, and $P < 0.05$ was considered significant.

TABLE 1. Characteristics of *db/db* and control littermate mice

	WT	*db/db*	*P* value
Body weight (g)			
4 wk	20.1 ± 1.9	20.8 ± 1.8	NS
9 wk	24.9 ± 1.9	41.2 ± 4.1	<0.0001
Body length (cm)	8.83 ± 0.17	8.33 ± 0.17	NS
BMI (body weight/height^2)	31.9 ± 0.19	59.3 ± 0.76	<0.01
Blood glucose (mg/dl)	124.8 ± 4.8	408.0 ± 20.6	<0.001
Plasma insulin (ng/ml)	1.31 ± 0.20	19.97 ± 3.46	<0.0001
Muscle weight (mg)			
Soleus	8.9 ± 1.1	6.6 ± 0.5	<0.05
EDL	10.0 ± 1.1	7.2 ± 0.5	<0.05
Plantaris	11.5 ± 0.8	9.1 ± 0.96	<0.05
Heart	103 ± 5	95 ± 4	<0.05
Muscle weight/body weight (ratio)			
Soleus	0.24 ± 0.02	0.12 ± 0.01	<0.001
EDL	0.32 ± 0.01	0.16 ± 0.01	<0.001
Plantaris	0.48 ± 0.02	0.21 ± 0.02	<0.001
Heart	5.15 ± 0.1	2.78 ± 0.1	<0.01

Average values of 12 *db/db* and 12 control mice are presented. NS, Not significant.

Results

Muscle atrophy is accelerated in db/db, insulin-resistant mice

The body weights of *db/db* mice were similar to those of littermate WT control mice at 4 wk age (Table 1), but after 9 wk, their weight was 65% greater (n = 12; $P < 0.0001$). At 9 wk of age, the blood sugar of *db/db* mice was 3.27-fold higher and plasma insulin levels were 15.5-fold higher than values in control mice (both n = 12; $P < 0.0001$).

Even though body weight was greater, muscle mass in *db/db* mice was reduced; the soleus (predominately oxidative, red fibers), EDL (predominately glycolytic, white fibers), and plantaris (mixed red and white fibers) muscles weighed significantly less than these muscles in control mice (−26, −28, and −21%, respectively; Table 1; n = 9; $P < 0.05$). Likewise, the ratio between the muscle weight and body weight in *db/db* mice was 50% below that of control mice ($P < 0.001$). The lower muscle mass of *db/db* mice at 70 d is shown in Fig. 1.

We also evaluated the cross-sectional area of gastrocnemius muscles containing both red and white fibers. As shown in Fig. 1B, the cross-sectional area of muscle fibers in *db/db* mice (1407.7 ± 61.5 μm^2) was significantly smaller than that in WT mice (2194.8 ± 106.3 μm^2; $P < 0.001$; n = 9).

Muscle atrophy in db/db mice is associated with increased protein degradation

The rate of protein degradation in the soleus muscle of *db/db* mice was 28.1% higher than the rate measured in soleus muscles of control mice. Protein degradation in EDL muscles of *db/db* mice was 43.5% higher and the rate in plantaris muscles was 34.1% higher than that in muscle of control mice (Fig. 2A; n = 9; $P < 0.05$).

To determine whether the increase in muscle proteolysis was related to activation of the UPP in *db/db* mice, we isolated proteasomes from gastrocnemius muscles and measured their activity. The proteasome chymotryptic-like peptidase activity was significantly increased (Fig. 2B; $P < 0.05$; n = 6).

Caspase-3 acts as an initial protease to cleave actomyosin/myofibrils, forming substrates that are rapidly degraded by the UPP (18). Activated caspase-3 in muscle also leaves a characteristic 14-kDa actin fragment as a footprint. The density of the 14-kDa actin fragment in gastrocnemius muscles of *db/db* mice was 2.1-fold higher, indicating that caspase-3 had cleaved actomyosin/myofibrils (Fig. 2C).

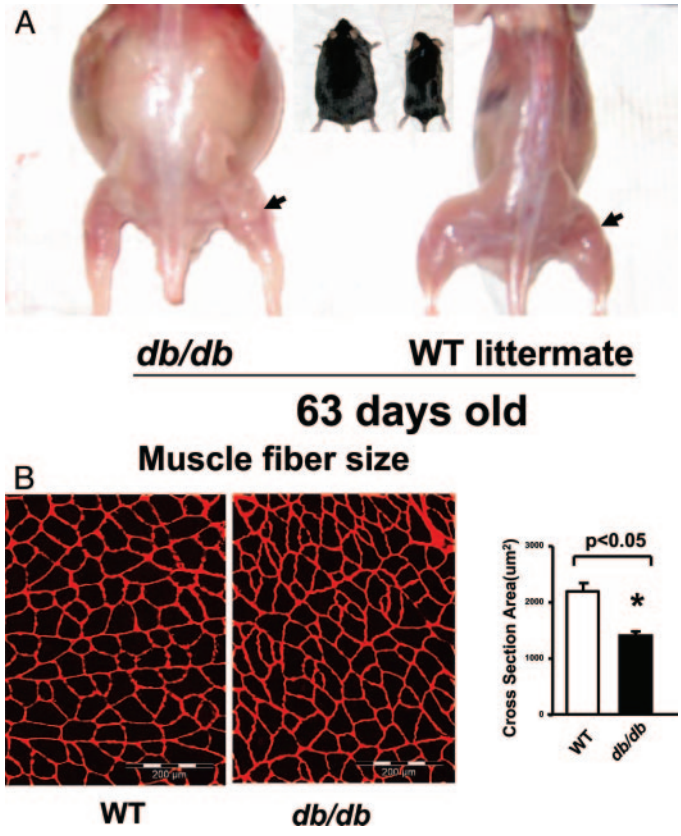

FIG. 1. Loss of muscle mass in *db/db* mice. A, Representative image showing differences in body weight and leg muscles of obese, *db/db* and littermate, WT control mice measured at d 63; B, cross-section of plantaris muscle showing the difference in myofiber size between obese *db/db* and control mice. The average size of myofibers from nine *db/db* and nine control mice is shown graphically; *, $P < 0.05$ difference.

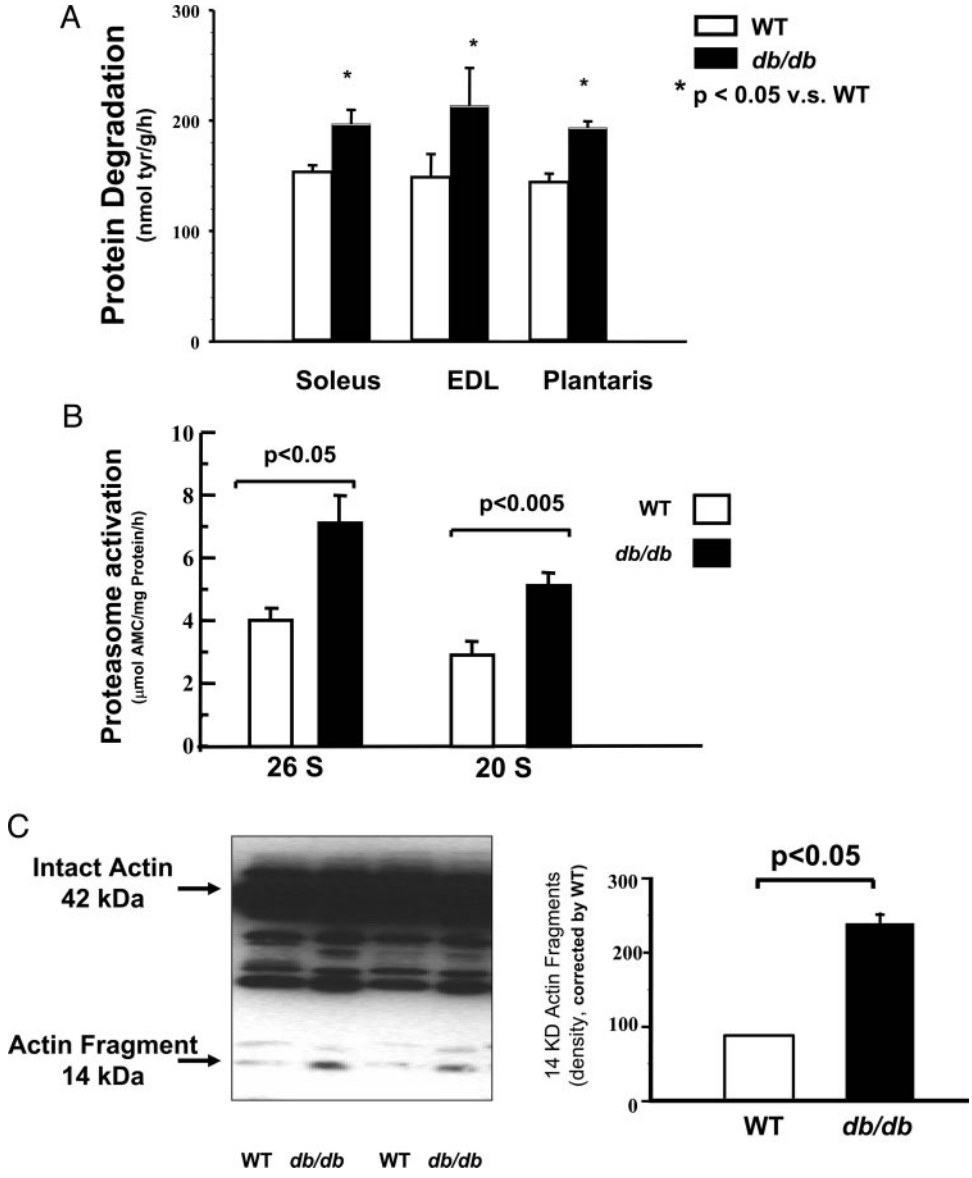

FIG. 2. Protein degradation is activated in muscles of obese *db/db* and control mice. A, Rates of protein degradation in the oxidative red-fiber soleus, the glycolytic white-fiber EDL, and the mixed-fiber plantaris muscle are shown. The rate was higher in all three types of muscles in nine *db/db* compared with nine control mice. B, Activities of the 20S and 26S proteasomes in gastrocnemius muscles of *db/db* and control mice; both activities are significantly increased in *db/db* mice. C, Density of the 14-kDa actin fragment in gastrocnemius muscles resulting from the activation of caspase-3, corrected by dividing by the density of the fragment in muscle of WT mice. The fragment level in nine *db/db* mice was substantially higher than levels in muscle of nine control mice.

PI3K/Akt cellular signaling is impaired in muscle of db/db mice

IRS-1-associated PI3K activity was significantly depressed in muscle of *db/db* mice (Fig. 3A). The decrease in PI3K activity was accompanied by an increase in phosphorylation of IRS-1 at serine 307 (Fig. 3B). This change in serine phosphorylation has been linked to decreased insulin responses because of its interference with insulin receptor signaling (25, 26). The lower PI3K activity was also associated with a decrease in pAkt (Fig. 3B).

Improving insulin sensitivity blocks the loss of muscle mass in db/db mice

Administration of high-affinity ligands for peroxisome proliferator-activated receptors, the thiazolidinediones, to obese animal models of insulin resistance can substantially correct hyperglycemia and/or hyperinsulinemia (27). To determine whether rosiglitazone would also prevent the increase in muscle protein degradation in *db/db* mice, we mixed rosiglitazone (8 mg/kg·d) into the food of control and *db/db* mice and fed this mixture or the standard diet. After 35 d, hyperglycemia and hyperinsulinemia were corrected in rosiglitazone-fed *db/db* mice, reaching levels found in WT mice (Fig. 4). However, the weight gain was unaffected.

There was a 27.2% increase in the cross-sectional area of muscle in *db/db* mice fed rosiglitazone compared with untreated *db/db* mice, but this increase was not statistically significant (data not shown). The ratio of the muscle to body weights was lower with rosiglitazone administration but not statistically different. Rosiglitazone therapy improved intracellular signaling processes in muscle of *db/db* mice; there was an increase in PI3K activity, a decrease in phosphorylation of IRS-1 serine 307, and an increase in the amount of the pAkt (Fig. 5). These improvements in the PI3K/Akt pathway were associated with a decrease in the rate of protein degradation measured in isolated muscles (Fig. 6A). There

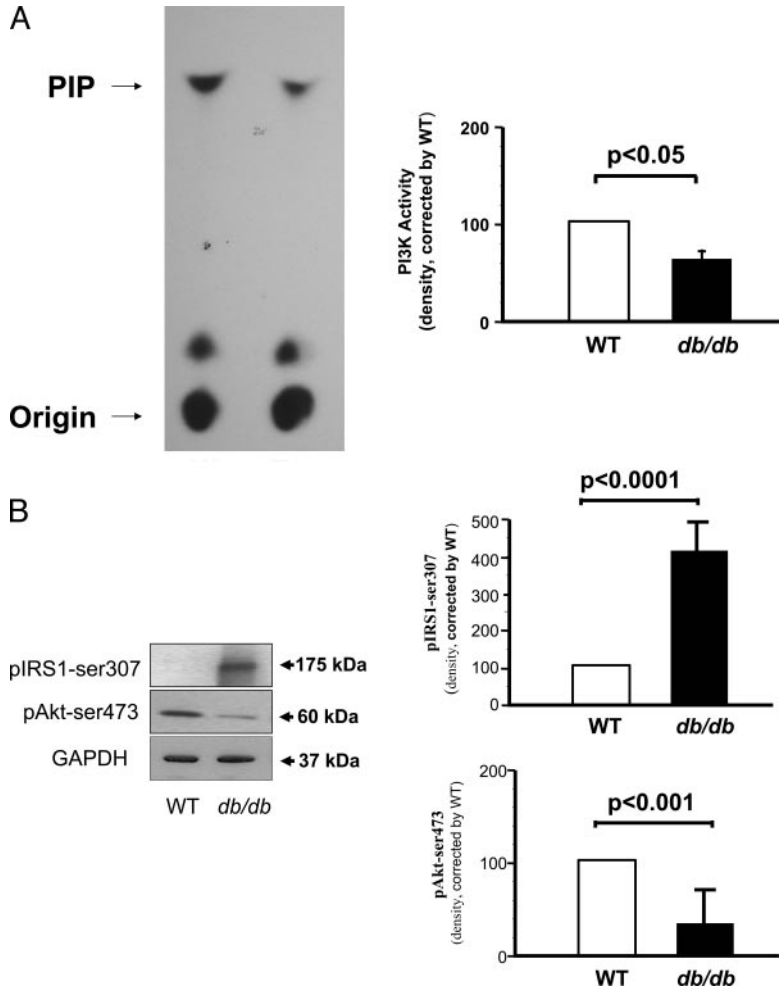

FIG. 3. The PI3K/Akt pathway is down-regulated in muscle of *db/db* mice. A, Results of IRS-1-associated PI3K activity in hind-limb muscles; it was lower in muscle of *db/db* mice. B, Western blots of IRS-1 that is phosphorylated on serine 307 and Akt phosphorylated on serine 473; GAPDH was used as a loading control. Serine 307 phosphorylation in gastrocnemius muscles of three *db/db* mice was associated with down-regulation of Akt activation compared with three control mice. PIP, Phosphatidylinositol phosphate.

also was a decrease in the proteolytic activity of the proteasome; the level in muscle of *db/db* mice was not significantly different from that measured in proteasomes isolated from control mice (Fig. 6B).

Rosiglitazone and potential processes that prevent muscle protein loss

To identify changes in underlying mechanisms influencing activation of protein degradation after administration of rosiglitazone, we studied changes in glucocorticoid production and circulating adiponectin levels. In catabolic conditions, we and others have found that glucocorticoids are essential for the activation of the UPP and protein degradation in muscle (12, 28–31). There was a sharp increase in glucocorticoid production in *db/db* mice, and this was eliminated when they were treated with rosiglitazone (Fig. 7A).

Adiponectin is produced in adipose cells and has been shown to suppress production of inflammatory adipokines

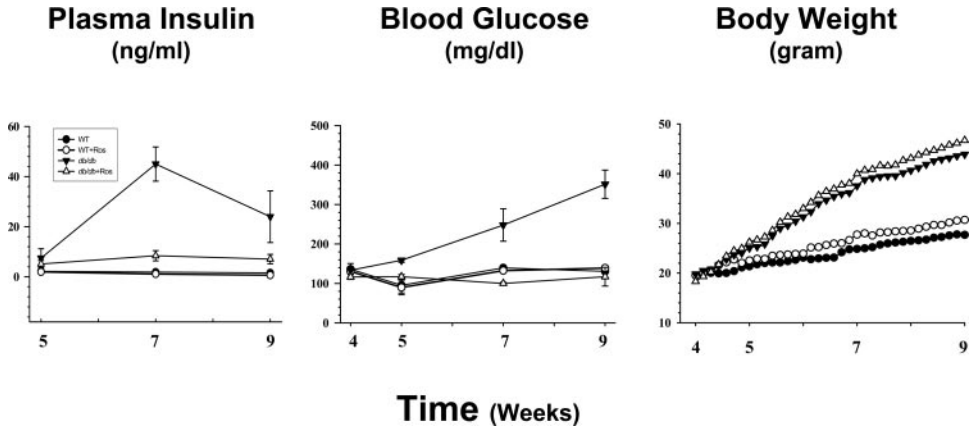

FIG. 4. Rosiglitazone (Ros) treatment improves insulin sensitivity but body weight remains higher in six *db/db* mice compared with values in six control mice.

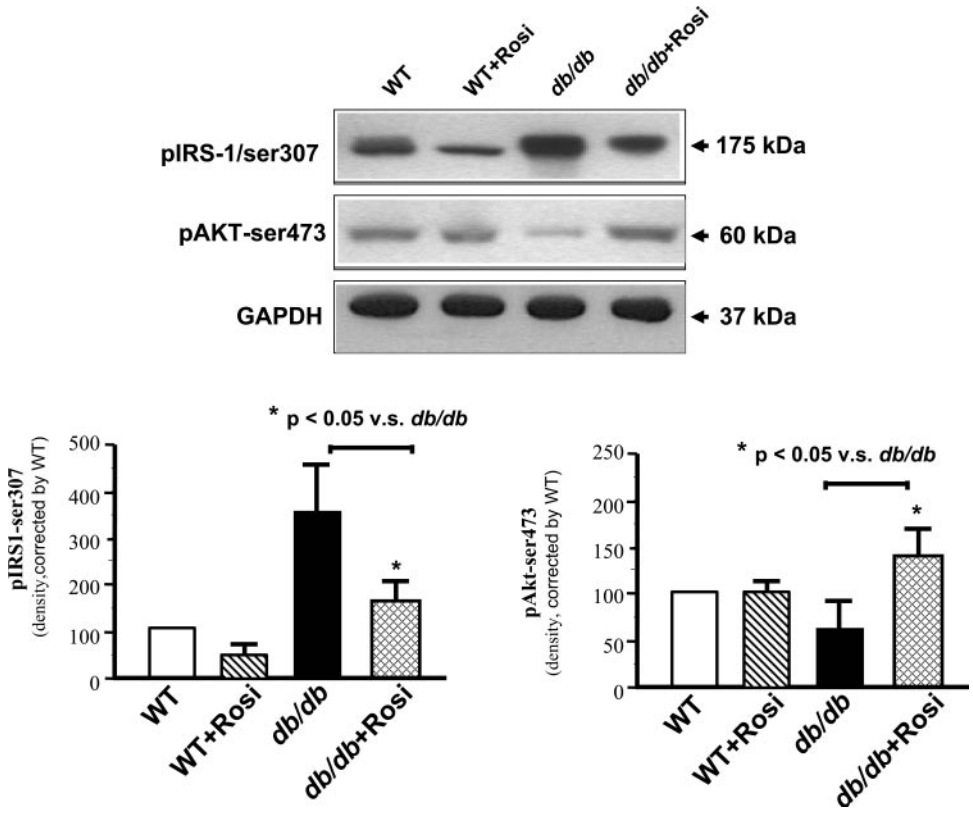

FIG. 5. Rosiglitazone (Rosi) treatment suppresses phosphorylation of serine 307 on IRS-1 and increases phosphorylation of Akt in gastrocnemius muscle of six *db/db* and six littermate control mice. Representative Western blots are shown with GAPDH used as a loading control.

(27). As expected, *db/db* mice had lower levels of adiponectin (Fig. 7B). Administration of rosiglitazone for 35 d resulted in an increase in plasma adiponectin levels in both *db/db* and control mice. Because the balance between adiponectin and cytokines is associated with insulin resistance (32), we treated differentiated 3T3-L1 cells with rosiglitazone for 16 h and measured mRNAs of adiponectin, TNFα, and IL-6. As shown in Fig. 8, rosiglitazone increased adiponectin mRNA by 31% but decreased the mRNAs of the inflammatory cytokines TNFα and IL-6 by 34 and 20%, respectively. The improvement in the high rate of muscle proteolysis was accompanied by an increase in the muscle content of pFoxO1, a decrease in FoxO1, and a decrease in the expression of the E3 ubiquitin-conjugating enzymes atrogin-1/MAFbx and MuRF1 (Fig. 9).

Discussion

Alarming predictions that the worldwide prevalence of diabetes mellitus will double in the next decade have emphasized that type 2 diabetes is associated with obesity and insulin resistance (33). Patients with type 2 diabetes are at increased risk for CKD and cardiovascular disease and potentially other problems (33, 34). For example, CKD patients with type 2 diabetes have evidence of accelerated loss of lean body mass that is linked to increased protein breakdown in muscle, but it is unclear whether type 2 diabetic patients without CKD also have accelerated muscle loss (35–37). On the other hand, there are reports indicating that whole-body protein flux in type 2 diabetic patients who have plasma insulin levels less than 120 pmol/liter is normal (38, 39). Perhaps type 2 diabetic patients with more severe insulin resistance or those with complicating disorders such as CKD may have an increase in muscle protein degradation. For example, CKD stimulates the loss of muscle protein in type 2 diabetic patients, and even mild degrees of CKD can cause insulin resistance (14, 35, 36). Hence, the degree of insulin resistance in type 2 diabetic patients could be aggravated by CKD. The present results are consistent with our findings in another model of insulin resistance, uremia (22, 40). In this model as well, we find that PI3K activity in muscle is depressed and protein degradation is accelerated. Thus, our results indicate that insulin resistance alone can increase muscle protein breakdown by suppressing PI3K activity.

The model of insulin resistance we studied, *db/db* mice, did not have complicating illnesses or differences in the duration of diabetes, exercise, *etc.*, but their muscles weighed less than those of the control mice and there was an increase in protein degradation (Figs. 1 and 2). There also were abnormalities in the cellular signaling pathway that stimulates muscle protein breakdown (17, 19, 20). Specifically, we found an increase in phosphorylation of serine 307 of IRS-1, a decrease in the activity of PI3K, and a decrease in pAkt (Fig. 3). These changes were associated with evidence of increased proteolytic activities of both caspase-3 and the UPP (Figs. 2 and 9). Although these changes in PI3K/Akt signaling are consistent with abnormalities we have found to cause accelerated muscle atrophy in streptozotocin-treated rats (17), there are differences in the two models. First, the level of phosphorylated serine 307 of IRS-1 was much higher in muscle of *db/db* mice. Second, potential toxicity from streptozotocin was not present in *db/db* mice (41). Because *db/db* mice are routinely used as a model of type 2 diabetes, our results seem physiologically relevant. Finally, our results indicate

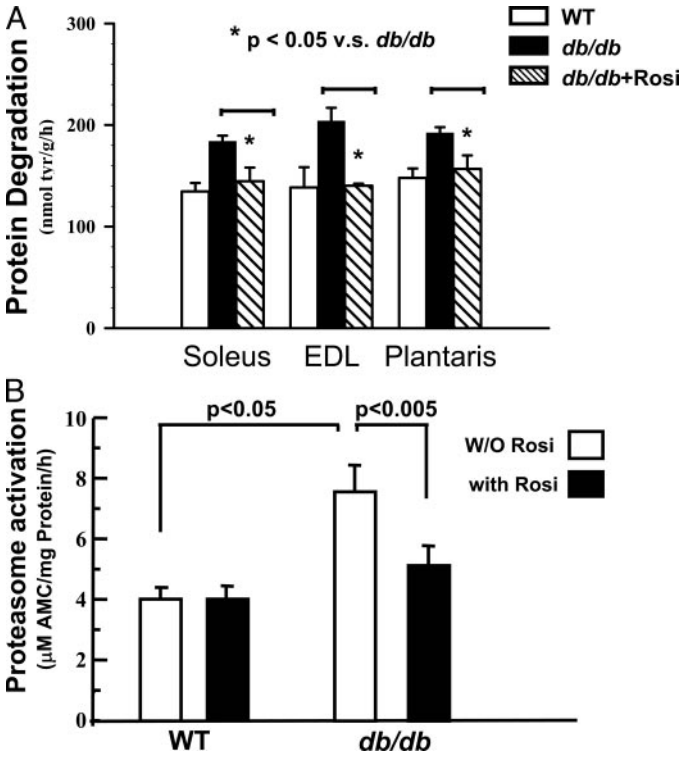

FIG. 6. Rosiglitazone (Rosi) treatment decreases protein degradation and proteasome activity in muscle of six *db/db* compared with six control mice. A, Rates of protein degradation in the soleus, EDL, and plantaris muscles are shown. The rate was lower in muscles of rosiglitazone-treated *db/db* mice. B, Activities of the proteasome in hind-limb muscles of *db/db* and control mice. The activity of the 26S proteasome was reduced by rosiglitazone treatment in muscles of *db/db* mice.

there is a common set of abnormalities of the PI3K/Akt pathway that leads to muscle wasting.

Our results demonstrate a cause-effect relationship between insulin resistance and the stimulation of muscle protein degradation. Specifically, we found that with rosiglitazone, blood glucose and plasma insulin levels fell sharply, indicating an improvement in insulin resistance. Concomitantly, the abnormalities in cellular signaling were corrected and proteasome proteolytic activity decreased (Figs. 5 and 6). However, there was only partial recovery of the cross-sectional area and mass of muscle. Possibly, the recovery was not complete because rosiglitazone did not stimulate protein synthesis. Indeed, it has been reported that changes in protein synthesis and degradation in response to changes in amino acids can differ even though both processes act through a common cell signaling pathway (42).

Mechanisms that could cause the abnormalities in cellular signaling leading to accelerated muscle protein degradation include increased glucocorticoid production and a decrease in the adiponectin level. An increase in glucocorticoids can stimulate the expression of atrogin-1/MAFbx and MuRF1 by increasing phosphorylation of the forkhead transcription factor (17, 19, 20). Moreover, we have shown that both a high physiological amount of glucocorticoids and either insulin deficiency or acidosis are required to activate the UPP and protein degradation in muscle of adrenalectomized rats; the same dose of glucocorticoids does not cause these abnormalities in rats without acidosis or insulin deficiency (12, 28). In the present study, we found that glucocorticoid production by *db/db* mice was high and that rosiglitazone eliminated this response. In addition, rosiglitazone reduced the activation of FoxO1 and the expression of atrogin-1/MAFbx and MuRF1 (Fig. 9). These results are consistent with the suppression of muscle protein degradation.

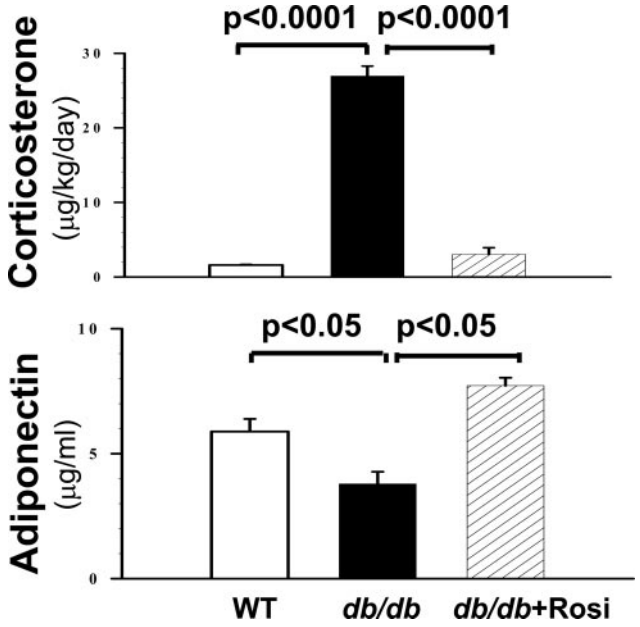

FIG. 7. Rosiglitazone (Rosi) treatment of four *db/db* and four control mice reduces their production of corticosterone and increases their circulating levels of adiponectin.

Regarding adiponectin, low levels have been shown to be closely linked to the development of insulin resistance via a mechanism involving enhanced cytokine production by adipocytes (32). In the present study, we showed that rosiglitazone increased plasma adiponectin levels (Fig. 7B) and decreased the expression of the mRNA levels of the inflammatory cytokines TNFα and IL-6 in adipocytes (Fig. 8). From these results, we cannot determine the contribution of inflammatory cytokines to insulin resistance, but others have shown that these cytokines are linked to the development of insulin resistance via phosphorylation of serine 307 of IRS-1 (9, 10).

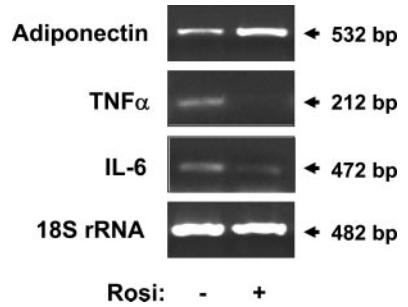

FIG. 8. Rosiglitazone treatment increases the mRNA level of adiponectin but decreases the levels of TNFα and IL-6 mRNAs in cultured, differentiated adipocytes. Representative image from RT-PCR is shown with the 18S RNA used as an internal control. The experiment was repeated three times.

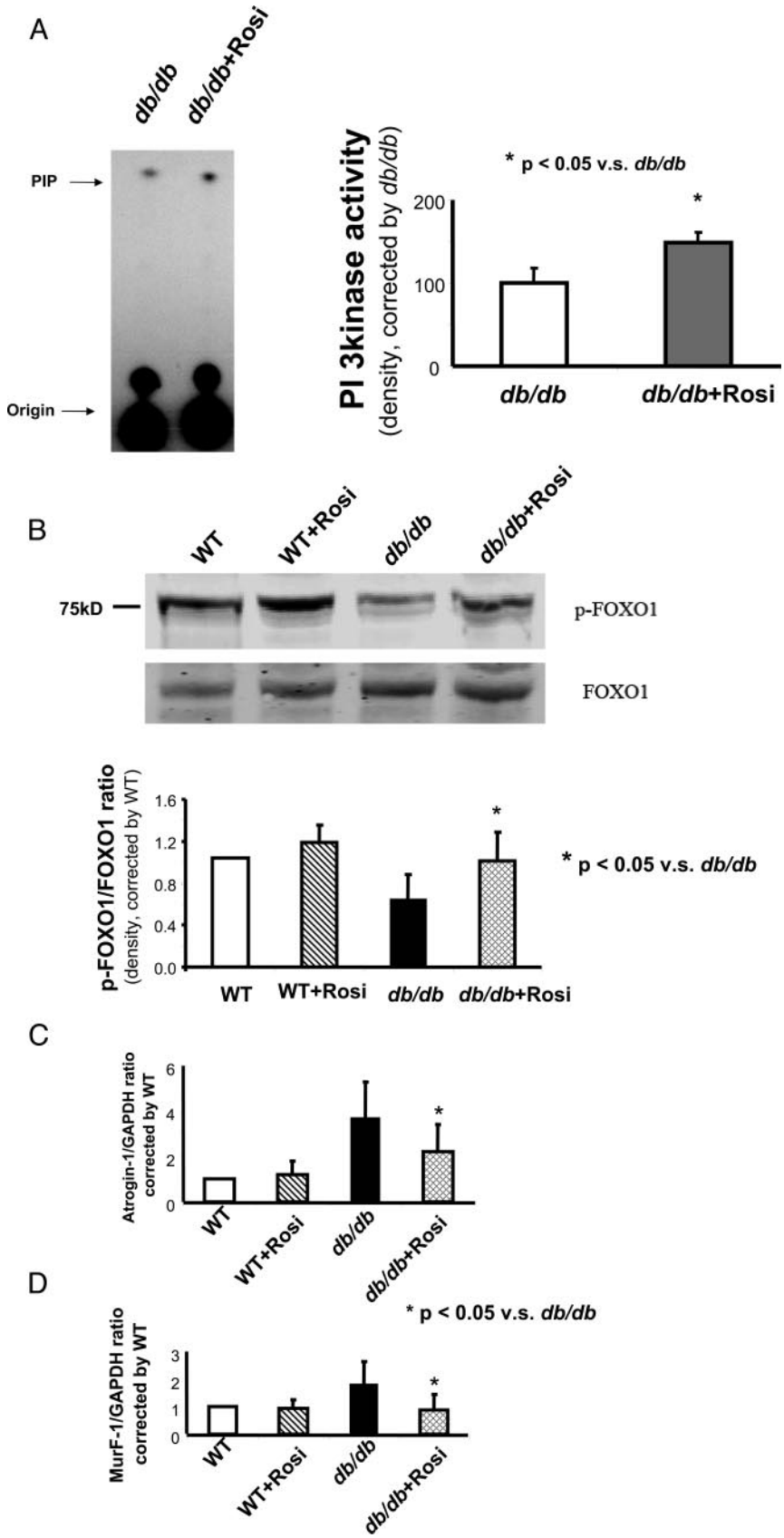

FIG. 9. Rosiglitazone (Rosi) treatment increases the activity of PI3K (A) and the phosphorylation of the forkhead transcription factor FoxO1 (B) and suppresses mRNA expression of the E3 ubiquitin-conjugating enzymes atrogin-1/MAFbx (C) and MuRF1 (D). The latter were measured by real-time PCR and corrected for values of GAPDH mRNA. Shown is the ratio of values of FoxO1 and pFoxO1 corrected for the ratio found in muscle of WT mice.

In conclusion, we find that insulin resistance is associated with accelerated muscle protein degradation in studies of a model of insulin resistance that is uncomplicated by kidney failure, sepsis, *etc.* The cellular signaling mechanism that links insulin resistance directly to protein degradation in muscle is also present in other conditions such as kidney failure. Consequently, the increase in muscle wasting that occurs in conditions associated with insulin resistance could arise in part from defects in cellular signaling caused by insulin resistance.

Acknowledgments

Received February 23, 2006. Accepted June 2, 2006.

Address all correspondence and requests for reprints to: Xiaonan Wang, M.D., Renal Division, WMB 338, Emory University School of Medicine, M/S 1930/001/1AG, 1639 Pierce Drive, Atlanta, Georgia 30322. E-mail: xwang03@emory.edu.

This study was supported by American Diabetes Association Junior Faculty Award 1-04-JF-48 and National Institutes of Health (NIH) R21 Grant DK62796 to X.H.W., NIH HL70762 to J.D., and NIH R01 DK 37175 and NIH P50 DK064233 to W.E.M.

References

1. **Griffiths RD** 1996 Muscle mass, survival, and the elderly ICU patient. Nutrition 12:456–458
2. **Windsor JA, Hill GL** 1988 Risk factors for postoperative pneumonia. The importance of protein depletion. Ann Surg 208:209–214
3. **Suttmann U, Ockenga J, Selberg O, Hoogestraat L, Deicher H, Muller MJ** 1995 Incidence and prognostic value of malnutrition and wasting in human immunodeficiency virus-infected outpatients. J Acquir Immune Defic Syndr Hum Retrovirol 8:239–246
4. **Wang AY, Sea MM, Tang N, Sanderson JE, Lui SF, Li PK, Woo J** 2004 Resting energy expenditure and subsequent mortality risk in peritoneal dialysis patients. J Am Soc Nephrol 15:3134–3143
5. **Mitch WE, Goldberg AL** 1996 Mechanisms of muscle wasting. The role of the ubiquitin-proteasome pathway. N Engl J Med 335:1897–1905
6. **Kimmel PL, Phillips TM, Simmens SJ, Peterson RA, Weihs KL, Alleyne S, Cruz I, Yanovski JA, Veis JH** 1998 Immunologic function and survival in hemodialysis patients. Kidney Int 54:236–244
7. **Bruunsgaard H, Pedersen M, Pedersen BK** 2001 Aging and proinflammatory cytokines. Curr Opin Hematol 8:131–136
8. **Stentz FB, Umpierrez GE, Cuervo R, Kitabchi AE** 2004 Proinflammatory cytokines, markers of cardiovascular risks, oxidative stress, and lipid peroxidation in patients with hyperglycemic crises. Diabetes 53:2079–2086
9. **Hotamisligil GS, Peraldi P, Budavari A, Ellis R, White MF, Spiegelman BM** 1996 IRS-1-mediated inhibition of insulin receptor tyrosine kinase activity in TNF-α- and obesity-induced insulin resistance. Science 271:665–668
10. **Rui L, Aguirre V, Kim JK, Shulman GI, Lee A, Corbould A, Dunaif A, White MF** 2001 Insulin/IGF-1 and TNF-α stimulate phosphorylation of IRS-1 at inhibitory Ser307 via distinct pathways. J Clin Invest 107:181–189
11. **Price SR, Bailey JL, Wang X, Jurkovitz C, England BK, Ding X, Phillips LS, Mitch WE** 1996 Muscle wasting in insulinopenic rats results from activation of the ATP-dependent, ubiquitin-proteasome proteolytic pathway by a mechanism including gene transcription. J Clin Invest 98:1703–1708
12. **Mitch WE, Bailey JL, Wang X, Jurkovitz C, Newby D, Price SR** 1999 Evaluation of signals activating ubiquitin-proteasome proteolysis in a model of muscle wasting. Am J Physiol 276:C1132–C1138
13. **Dardevet D, Sornet C, Attaix D, Baracos VE, Grizard J** 1994 Insulin-like growth factor-1 and insulin resistance in skeletal muscles of adult and old rats. Endocrinology 134:1475–1484
14. **Kobayashi S, Maesato K, Moriya H, Ohtake T, Ikeda T** 2005 Insulin resistance in patients with chronic kidney disease. Am J Kidney Dis 45:275–280
15. **DeFronzo RA, Beckles AD** 1979 Glucose intolerance following chronic metabolic acidosis in man. Am J Physiol 236:E328–E334
16. **Hasselgren PO, Warner BW, James JH, Takehara H, Fischer JE** 1987 Effect of insulin on amino acid uptake and protein turnover in skeletal muscle from septic rats. Evidence for insulin resistance of protein breakdown. Arch Surg 122:228–233
17. **Lee SW, Dai G, Hu Z, Wang X, Du J, Mitch WE** 2004 Regulation of muscle protein degradation: coordinated control of apoptotic and ubiquitin-proteasome systems by phosphatidylinositol 3 kinase. J Am Soc Nephrol 15:1537–1545
18. **Du J, Wang X, Miereles C, Bailey JL, Debigare R, Zheng B, Price SR, Mitch WE** 2004 Activation of caspase-3 is an initial step triggering accelerated muscle proteolysis in catabolic conditions. J Clin Invest 113:115–123
19. **Sandri M, Sandri C, Gilbert A, Skurk C, Calabria E, Picard A, Walsh K, Schiaffino S, Lecker SH, Goldberg AL** 2004 Foxo transcription factors induce the atrophy-related ubiquitin ligase atrogin-1 and cause skeletal muscle atrophy. Cell 117:399–412
20. **Stitt TN, Drujan D, Clarke BA, Panaro F, Timofeyva Y, Kline WO, Gonzalez M, Yancopoulos GD, Glass DJ** 2004 The IGF-1/PI3K/Akt pathway prevents expression of muscle atrophy-induced ubiquitin ligases by inhibiting FOXO transcription factors. Mol Cell 14:395–403
21. **Lecker SH, Jagoe RT, Gilbert A, Gomes M, Baracos V, Bailey J, Price SR, Mitch WE, Goldberg AL** 2004 Multiple types of skeletal muscle atrophy involve a common program of changes in gene expression. FASEB J 18:39–51
22. **Bailey JL, Wang X, England BK, Price SR, Ding X, Mitch WE** 1996 The acidosis of chronic renal failure activates muscle proteolysis in rats by augmenting transcription of genes encoding proteins of the ATP-dependent ubiquitin-proteasome pathway. J Clin Invest 97:1447–1453
23. **Clark AS, Mitch WE** 1983 Comparison of protein synthesis and degradation in incubated and perfused muscle. Biochem J 212:649–653
24. **Solomon V, Goldberg AL** 1996 Importance of the ATP-ubiquitin-proteasome pathway in the degradation of soluble and myofibrillar proteins in rabbit muscle extracts. J Biol Chem 271:26690–26697
25. **Tanti JF, Gremeaux T, van Obberghen E, Le Marchand-Brustel Y** 1994 Serine/threonine phosphorylation of insulin receptor substrate 1 modulates insulin receptor signaling. J Biol Chem 269:6051–6057
26. **Aguirre V, Werner ED, Giraud J, Lee YH, Shoelson SE, White MF** 2002 Phosphorylation of Ser307 in insulin receptor substrate-1 blocks interactions with the insulin receptor and inhibits insulin action. J Biol Chem 277:1531–1537
27. **Saltiel AR, Olefsky JM** 1996 Thiazolidinediones in the treatment of insulin resistance and type II diabetes. Diabetes 45:1661–1669
28. **Price SR, England BK, Bailey JL, Van Vreede K, Mitch WE** 1994 Acidosis and glucocorticoids concomitantly increase ubiquitin and proteasome subunit mRNAs in rat muscle. Am J Physiol 267:C955–C960
29. **Wing SS, Goldberg AL** 1993 Glucocorticoids activate the ATP-ubiquitin-dependent proteolytic system in skeletal muscle during fasting. Am J Physiol 264:E668–E676
30. **Hall-Angeras M, Angeras U, Zamir O, Hasselgren PO, Fischer JE** 1991 Effect of the glucocorticoid receptor antagonist RU 38486 on muscle protein breakdown in sepsis. Surgery 109:468–473
31. **Song YH, Li Y, Du J, Mitch WE, Rosenthal N, Delafontaine P** 2005 Muscle-specific expression of IGF-1 blocks angiotensin II-induced skeletal muscle wasting. J Clin Invest 115:451–458
32. **Maeda N, Shimomura I, Kishida K, Nishizawa H, Matsuda M, Nagaretani H, Furuyama N, Kondo H, Takahashi M, Arita Y, Komuro R, Ouchi N, Kihara S, Tochino Y, Okutomi K, Horie M, Takeda S, Aoyama T, Funahashi T, Matsuzawa Y** 2002 Diet-induced insulin resistance in mice lacking adiponectin/ACRP30. Nat Med 8:731–737
33. **King H, Aubert RE, Herman WH** 1998 Global burden of diabetes, 1995–2025: prevalence, numerical estimates, and projections. Diabetes Care 21:1414–1431
34. **Jones CA, Krolewski AS, Rogus J, Xue JL, Collins A, Warram JH** 2005 Epidemic of end-stage renal disease in people with diabetes in the United States population: do we know the cause? Kidney Int 67:1684–1691
35. **Pupim LB, Heimburger O, Qureshi AR, Ikizler TA, Stenvinkel P** 2005 Accelerated lean body mass loss in incident chronic dialysis patients with diabetes mellitus. Kidney Int 68:2368–2374
36. **Pupim LB, Flakoll PJ, Majchrzak KM, Aftab Guy DL, Stenvinkel P, Ikizler TA** 2005 Increased muscle protein breakdown in chronic hemodialysis patients with type 2 diabetes mellitus. Kidney Int 68:1857–1865
37. **Chevalier S, Burgess SC, Malloy CR, Gougeon R, Marliss EB, Morais JA** 2006 The greater contribution of gluconeogenesis to glucose production in obesity is related to increased whole-body protein catabolism. Diabetes 55:675–681
38. **Halvatsiotis P, Short KR, Bigelow M, Nair KS** 2002 Synthesis rate of muscle proteins, muscle functions, and amino acid kinetics in type 2 diabetes. Diabetes 51:2395–2404
39. **Petersen KF, Hendler R, Price T, Perseghin G, Rothman DL, Held N, Amatruda JM, Shulman GI** 1998 $^{13}C/^{31}P$ NMR studies on the mechanism of insulin resistance in obesity. Diabetes 47:381–386
40. **Bailey JL, Zheng B, Hu Z, Price SR, Mitch WE** 2006 Chronic kidney disease causes defects in signaling through the insulin receptor substrate/phosphatidylinositol 3-kinase/Akt pathway: implications for muscle atrophy. J Am Soc Nephrol 17:1388–1394
41. **Wold LE, Ren J** 2004 Streptozotocin directly impairs cardiac contractile function in isolated ventricular myocytes via a p38 MAP kinase-dependent oxidative stress mechanism. Biochem Biophys Res Commun 318:1066–1071
42. **Kanazawa T, Taneike I, Akaishi R, Yoshizawa F, Furuya N, Fujimura S, Kadowaki M** 2004 Amino acids and insulin control autophagic proteolysis through different signaling pathways in relation to mTOR in isolated rat hepatocytes. J Biol Chem 279:8452–8459